Inorg. Chem. **2002**, *41*, 1048–1055

High-Resolution Optical Spectroscopy of $Na_3[Ln(dpa)_3]\cdot 13H_2O$ with Ln = Er^{3+}, Tm^{3+}, Yb^{3+}

Christine Reinhard and Hans U. GUdel*

Departement für Chemie und Biochemie, Universität Bern, Freiestrasse 3, CH-3000 Bern 9, Switzerland

Received August 6, 2001

The title compounds were synthesized and studied by solution and single-crystal absorption, luminescence, and excitation spectroscopy. The f–f luminescence is induced in the Tm^{3+} and Yb^{3+} complexes in solution by exciting into the $^1\Pi$–$^1\Pi^*$ absorptions of the ligand in the UV. A single-configurational coordinate model is proposed to rationalize the nonradiative relaxation step from ligand-centered to metal-centered excited states in $[Yb(dpa)_3]^{3-}$ (dpa = 2,6-pyridinedicarboxylate). Direct f–f excitation is used in crystals of $Na_3[Tm(dpa)_3]\cdot 13H_2O$ and $Na_3[Yb(dpa)_3]\cdot 13H_2O$ to induce f–f luminescence. From low-temperature, high-resolution absorption, luminescence, and excitation spectra, the ligand-field splittings in the relevant states can be determined. It was impossible to induce NIR to VIS upconversion in any of the complexes. This is mainly due to the fact that nonradiative relaxation among the f–f excited states is highly competitive, even in $[Yb(dpa)_3]^{3-}$ with an energy gap between $^2F_{5/2}$ and $^2F_{7/2}$ of about 10000 cm^{-1}. It can be rationalized on the basis of an adapted energy gap law. No luminescence at all could be detected in $Na_3[Er(dpa)_3]\cdot 13H_2O$.

1. Introduction

The optical and spectroscopic properties of lanthanide containing compounds are of enormous interest in various areas of science and technology. Interestingly, there seem to exist two relatively distinct areas with rather limited communication. One could be called the chemical area, in which molecular lanthanide complexes are being prepared and investigated.[1] The physical area is focused on lanthanide doped ionic crystals or glasses.[2]

The luminescence properties of lanthanide complexes are usually studied in solution. Low-resolution spectroscopy, combined with lifetime and quantum yield measurements, is the principal technique. Questions of light conversion, that is, energy transfer from the ligand to metal localized excited states, are being studied. Many attempts are being made to increase the light output, that is, the quantum yield, by chemically varying the ligand coordination and the solvent.[3,4] The big majority of these studies has been on Tb^{3+} (green emitter) and Eu^{3+} (red emitter) complexes, with an increasing interest in recent years in Yb^{3+} complexes.[5−7] The application potential of these systems is in areas where chemical solubility or chemical attachment is important: luminescent probes in analytical and biomedical imaging applications.[8] The principal problem in all molecular lanthanide complexes with organic ligands is that spontaneous light emission is in very strong competition with nonradiative relaxation processes involving the high-energy ligand and solvent vibrations. Deuteration, fluorination, and encapsulation are standard techniques to counter this problem. Another issue of importance is the thermodynamic, kinetic, and photochemical stability of such complexes.

In lanthanide doped oxide or halide crystals and glasses, the highest vibrational energies and, thus, the efficiency of

* Author to whom correspondence should be addressed. E-mail: hans-ulrich.guedel@iac.unibe.ch. Fax: +41 31 631 43 99.

(1) Sabbatini, N.; Guardigli, M.; Manet, I. *Handbook on the Physics and Chemistry of Rare Earths*; Elsevier Science: New York, 1996; Vol. 23.
(2) Fejer, M. M.; Injeyan, H.; Keller, U. *Trends in Optics and Photonics*; Optical Society of America: Washington, DC, 1999; Vol. 26.
(3) Hasegawa, Y.; Takashi, O.; Sogabe, K.; Kawamura, Y.; Wada, Y.; Nakashima, N.; Yanagida, S. *Angew. Chem.* **2000**, *112*, 365−368.
(4) Beeby, A.; Clarkson, I. M.; Dickins, R. S.; Faulkner, S.; Parker, D.; Royle, L.; de Sousa, A. S.; Williams, J. A. G.; Woods, M. *J. Chem. Soc., Perkin Trans. 2* **1999**, 493−503.
(5) Maupin, L. C.; Dickins, R. S.; Govenlock, L. G.; Mathieu, C. E.; Parker, D.; Williams, J. A. G.; Riehl, J. P. *J. Phys. Chem. A* **2000**, *104*, 6709−6717.
(6) Beeby, A.; Dickins, R. S.; Faulkner, S.; Parker, D.; Williams, J. A. G. *Chem. Commun.* **1997**, 1401−1402.
(7) Klink, S. I.; Hebbink, G. A.; Grave, L.; Peters, F. G. A.; Van Veggel, F. C. J. M.; Reinhoudt, D. N.; Hofstraat, J. W. *Eur. J. Org. Chem.* **2000**, 1923−1931.
(8) Dickinson, E. F. G.; Pollak, A.; Diamandis, E. P. *J. Photochem. Photobiol. B.* **1995**, *27*, 3−19.

10.1021/ic0108484 CCC: $22.00
Published on Web 02/12/2002

multiphonon relaxation processes are much reduced. Spectroscopic studies on such systems are often done at cryogenic temperatures using high spectral resolution. Crystal-field splittings can, thus, be determined and analyzed in terms of theoretical models.[9] Both spontaneous and stimulated emissions of such materials are used in many technologically important applications. Spontaneous emission is the basis in lighting and display phosphors as well as scintillators.[10,11] Lanthanide doped crystals and glasses are among the most important laser materials with applications in imaging, medical, materials processing, analytical, environmental, and telecommunications areas.

We have shown that chemical variation can significantly change the light emission properties not only in molecular but also in ionic lanthanide compounds. Using very similar principles to the ones used for complexes, we have been able to reduce the efficiency of multiphonon relaxation processes in Er^{3+}, Tm^{3+}, Dy^{3+}, and Ho^{3+} doped crystals by choosing heavier halide lattices instead of the usual oxides and fluorides.[12−15] This can lead to new photophysics and, of particular interest to us, new near-IR (NIR) to visible (VIS) upconversion processes.

These chlorides and bromides are usually air-sensitive and hygroscopic. From a materials point of view, this is a serious disadvantage. In addition, energy transfer and migration processes usually dominate the excitation dynamics of doped ionic lattices, unless the doping concentration is very small. In principle, these disadvantages can be avoided in molecular complexes, both in solution and in the solid state.

In the present paper, our objective is threefold. What can we learn by applying high-resolution, single-crystal absorption and luminescence spectroscopy at cryogenic temperature of molecular complexes? Is it possible to induce photon upconversion in such a system? Is it possible to derive ligand-field energy splittings using our high-resolution techniques? The $^2F_{7/2}$ and $^2F_{5/2}$ splittings of Yb^{3+} are of particular interest in this respect. The Yb^{3+} ion plays a very special and important role because of its very simple f−f energy level structure: besides the $^2F_{7/2}$ ground multiplet, there is only the $^2F_{5/2}$ excited multiplet around 1 μm, with the rest of the NIR and VIS spectrum transparent. In ionic systems, Yb^{3+} is a very good sensitizer for upconversion processes, particularly in Tm^{3+} and Er^{3+} codoped crystals.[16] If upconversion could be achieved in molecular systems, dinuclear complexes containing Yb^{3+}−Tm^{3+} or Yb^{3+}−Er^{3+} pairs would provide ideal combinations. From numerous studies on various lanthanide ions, it is known that in the nine-coordinate $[Ln(dpa)_3]^{3-}$ complexes, where dpa = 2,6-pyridinedicarboxylate, relatively high quantum yields of the f−f emission compared to other complexes can be achieved. We therefore chose the $[Er(dpa)_3]^{3-}$, $[Tm(dpa)_3]^{3-}$, and $[Yb(dpa)_3]^{3-}$ complexes for this study.

2. Experimental Section

2.1. Synthesis.[17] $Na_3[Ln(dpa)_3]\cdot 13H_2O$ (Ln = Er^{3+}, Tm^{3+}, Yb^{3+}). The commercial Ln_2O_3 (Ln = Er^{3+} (99.999% Johnson Mattey & Brandenberger AG), Tm^{3+} (≥ 99.9% puriss., Fluka), and Yb^{3+} (99.99% Rhône-Poulenc Chimie, France)) was heated in an excess of 32% HCl until a clear solution had formed. The solution was evaporated to dryness and the residue redissolved in water. This lanthanide chloride solution was added to a hot aqueous solution of 2,6-pyridinedicarboxylic acid (99%, Aldrich) in a molar ratio of 1:3. The solution was brought to a pH of approximately 7.5 by the dropwise addition of a dilute NaOH solution. Single crystals of $Na_3[Ln(dpa)_3]\cdot 13H_2O$ (Ln = Er^{3+}, Tm^{3+}, Yb^{3+}) were obtained by slow evaporation of the solution within one week. These compounds all crystallize in rectangular plates with an average size of 2 mm × 2 mm × 1 mm. The crystals have the color of the respective lanthanide, which is pink in the case of erbium and colorless for the ytterbium and thulium compounds. They lose water quite easily when removed from the mother liquor.

$[Ln(dpa)_3]^{3-}$ Doped Polyvinyl Alcohol (PVA) Films. $Na_3[Ln(dpa)_3]\cdot 13H_2O$ (Ln = Er^{3+}, Tm^{3+}, Yb^{3+}) was dissolved in hot water. This solution was added to a hot aqueous solution of PVA (72000, Fluka). A thin film was obtained by pouring the mixture into a Petri dish and evaporating the solvent.

2.2. Crystal and Molecular Structure. $Na_3[Er(dpa)_3]\cdot 13H_2O$ crystallizes in the monoclinic space group $P2_1/c$ as described by Albertsson.[17] The structure is built up of mononuclear tris(2,6-pyridinedicarboxylate) complexes, which crystallize as Λ,Δ-racemates. The lanthanide ion is surrounded by six oxygen and three nitrogen atoms, which define a distorted tricapped trigonal prism. We used powder X-ray diffraction to characterize $Na_3[Ln(dpa)_3]\cdot 13H_2O$ (Ln = Er^{3+}, Tm^{3+}, Yb^{3+}). For the Er^{3+} compound, the published structure was verified by a Rietveld analysis of the powder diffraction pattern. The Tm^{3+} and Yb^{3+} compounds have completely analogous powder patterns, and we conclude that the three compounds are isostructural.

2.3. Spectroscopy. Absorption Measurements. All the crystal spectra were measured with unpolarized light and random crystal orientation. Absorption spectra were taken on a Cary 5e (Varian) spectrometer. Solid samples were mounted in a closed copper cell and cooled with a closed cycle cryostat (Air Products Displex).

Luminescence and Excitation Measurements. Continuous-wave luminescence and excitation spectra were measured using a Ti:sapphire laser (Spectra Physics 3900S), pumped by an argon ion laser (Spectra Physics 2060-10SA). Wavelength control was achieved by an inchworn driven (Burleigh PZ-501) birefringent filter, and the wavelength was monitored with a wavemeter (Burleigh WA2100). The sample luminescence was dispersed by a 0.85 m double monochromator (Spex 1402) and detected by a cooled photomultiplier tube (RCA C31034 or Hamamatsu 3310-01) using a photon counting system (Stanford Research SR400). Cooling of the solid samples was achieved using the helium gas flow technique. For Tm^{3+} lifetime measurements, rectangular pulses

(9) Lüthi, S. R.; Hehlen, M. P.; Quagliano, J. R.; Güdel, H. U. *Phys. Rev. B* **1998**, *57*, 15229−15241.
(10) Jüstel, T.; Nikol, H.; Ronda, C. *Angew. Chem.* **1998**, *110*, 3250−3271.
(11) Guillot-Noël, O.; de Haas, J. T. M.; Dorenbos, P.; van Eijk, C. W. E.; Krämer, K. W.; Güdel, H. U. *J. Lumin.* **1999**, *85*, 21−35.
(12) Hehlen, M. P.; Frei, G.; Güdel, H. U. *Phys. Rev. B* **1994**, *50*, 16264−16273.
(13) Riedener, T.; Krämer, K.; Güdel, H. U. *Inorg. Chem.* **1995**, *34*, 2745−2752.
(14) Wermuth, M.; Riedener, T.; Güdel, H. U. *Phys. Rev. B* **1998**, *57*, 4369−4376.
(15) Müller, P.; Wermuth, M.; Güdel, H. U. *Chem. Phys. Lett.* **1998**, *290*, 105−111.
(16) Heine, F.; Ostroumov, V.; Heumann, E.; Jensen, T.; Huber, G.; Chai, B. T. H. *OSA Proc. Adv. Solid-State Lasers* **1995**, *24*, 77.
(17) Albertsson, J. *Acta Chem. Scand.* **1972**, *26*, 985−1004.

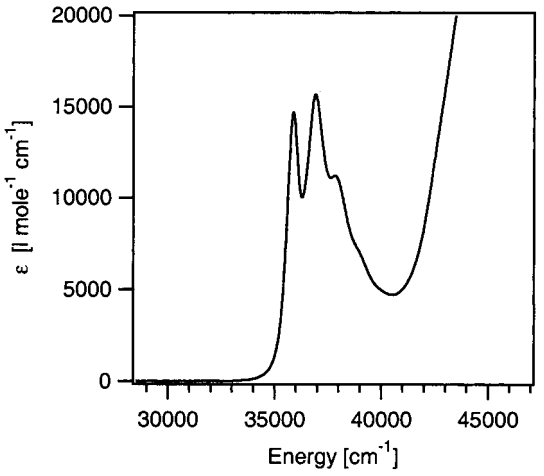

Figure 1. Absorption spectrum of a 0.14 mM aqueous solution of $[Yb(dpa)_3]^{3-}$ at room temperature. Value of ϵ is given per mole of the complex.

were generated by using an acousto-optic modulator (Coherent 305) connected to a function generator (Stanford Research DS 345). For the Yb^{3+} lifetime measurement, 10 ns pulses of a dye laser (Lambda Physik FL3002, Pyridine 1 in methanol) pumped by the second harmonic of a Nd:YAG (Quanta Ray DCR 3) were Raman-shifted (Quanta Ray, RS-1, H_2, 340 psi, operative range 935−1025 nm). The sample luminescence was dispersed by a 0.75 m single monochromator (Spex 1702) equipped with a 750 nm blazed 600 grooves/mm grating. The temporal behavior of the luminescence intensity was detected using a multichannel scaler (Stanford Research SR430) for decay curves. Luminescence spectra excited in the UV were measured using a Spex Fluorolog-3 (Jobin Yvon Ldt) system. All the spectra were corrected for the sensitivity of the detection systems. The wavelength was corrected for the refractive index of air (vacuum correction). The excitation spectra were corrected for the wavelength dependence of the output power of the Ti:sapphire laser and the xenon lamp, respectively.

3. Results

Figure 1 shows the absorption spectrum of a 0.14 mM aqueous solution of $[Yb(dpa)_3]^{3-}$ at room temperature in the near UV. It shows a very intense band system with an origin at 35870 cm^{-1} and progression members at 36900, 37850, and 39020 cm^{-1}. A shoulder of a further electronic transition can be estimated at 45400 cm^{-1}. The spectrum has the typical shape and position of a ligand-centered $^1\Pi-{}^1\Pi^*$ absorption band. Exciting an aqueous solution of $[Yb(dpa)_3]^{3-}$ in the UV at 37026 cm^{-1} leads to a broad band luminescence in the visible region with a maximum around 24320 cm^{-1}. As has been shown by Nudelman *et al.*, this emission stems from a photoproduct formed under UV illumination of the ligand. The ligand dpa is reported to exhibit only negligible fluorescence under these conditions.[18]

Figure 2 presents the high-resolution 12 K crystal absorption spectra of $Na_3[Ln(dpa)_3]\cdot 13H_2O$ (Ln = Er^{3+}, Tm^{3+}) in the range between 5000 and 33000 cm^{-1}. The sharp line multiplets are characteristic for the specific lanthanide ion and readily identified as f−f transitions on the basis of their

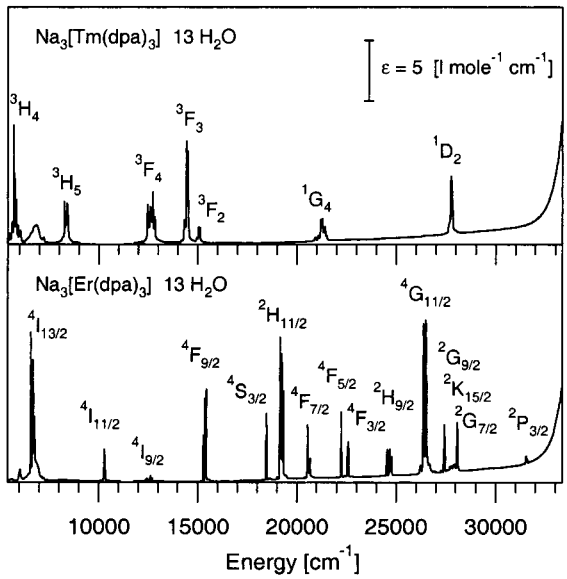

Figure 2. Unpolarized single-crystal survey absorption spectra of $Na_3[Ln(dpa)_3]\cdot 13H_2O$ (Ln = Er^{3+}, Tm^{3+}) at 12 K. All observed transitions are labeled with the respective $^{2S+1}L_J$ term symbol.

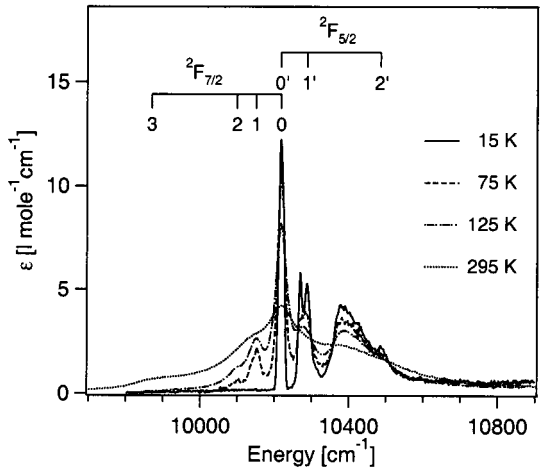

Figure 3. Unpolarized high-resolution absorption spectra at various temperatures of the $^2F_{7/2} \rightarrow {}^2F_{5/2}$ transition in a $Na_3[Yb(dpa)_3]\cdot 13H_2O$ single crystal. Electronic origins of the individual ligand-field levels are assigned at the top.

energies and shapes. The ligand field leads to the observed multiplet splittings. These absorption bands are readily assigned by a comparison with the Dieke diagram.[19] Above 30000 cm^{-1}, the crystal spectrum is dominated by the onset to the strong ligand-centered $^1\Pi-{}^1\Pi^*$ absorptions. Note that the *y* axis is scaled up by 3 orders of magnitude compared to that in Figure 1.

Figure 3 shows the temperature-dependent single-crystal absorption spectra of $Na_3[Yb(dpa)_3]\cdot 13H_2O$. The $^2F_{7/2} \rightarrow {}^2F_{5/2}$ transition is shown at various temperatures between 15 K and room temperature. The 15 K absorption spectrum shows three strong and sharp peaks at 10217, 10288, and 10485 cm^{-1} and a broad band between 10325 and 10700 cm^{-1}. Upon heating, two prominent peaks at 10150 and

(18) Nudelman, R.; Bronk, B. V.; Efrima, S. *Appl. Spectrosc.* **2000**, *54*, 445−449.

(19) Dieke, G. H. *Spectra and Energy Levels of Rare Earth Ions in Crystals*; Crosswhite, H. M., Crosswhite, H., Eds.; Interscience Publishers: New York, 1968.

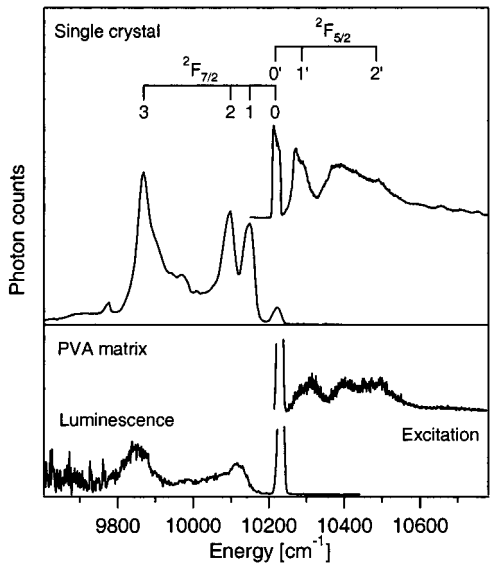

Figure 4. Luminescence and excitation spectra of the $^2F_{7/2} \leftrightarrow {}^2F_{5/2}$ transitions in a $Na_3[Yb(dpa)_3]\cdot 13H_2O$ single crystal and in a $[Yb(dpa)_3]^{3-}$ doped PVA matrix at 15 K. The excitation wavelength was 10515 cm^{-1} for both luminescence spectra. The luminescence was detected at 10152 cm^{-1} for the single crystal and at 10119 cm^{-1} for the PVA matrix.

10099 cm^{-1} emerge, because of transitions from thermally populated ligand-field levels of the ground state. The two brackets at the top indicate the ligand-field splittings in the ground ($^2F_{7/2}$) and excited ($^2F_{5/2}$) states derived from these spectra.

The 15 K luminescence and excitation spectra of a $Na_3[Yb(dpa)_3]\cdot 13H_2O$ single crystal and of a $[Yb(dpa)_3]^{3-}$ doped polyvinyl alcohol (PVA) matrix are shown in Figure 4. The fine structure is considerably better resolved in the crystal spectra. This is a result of inhomogeneous broadening effects in the plastic. The four well-resolved maxima at 10217, 10150, 10099, and 9869 cm^{-1} in the crystal luminescence spectrum are assigned to the electronic origins of transitions to the ligand-field levels of the ground state. The excitation spectrum closely follows the absorption spectrum, and the peaks are assigned accordingly. From a combination of absorption, luminescence, and excitation spectra, we thus have a consistent picture of the ligand-field splittings in both the ground and the excited states. From the coincidence of absorption and excitation spectra, we conclude that the luminescence is intrinsic, that is, from the bulk of the material. The $^2F_{7/2}(0) \rightarrow {}^2F_{5/2}(0')$ transitions exhibit a great deal of vibrational sideband intensity, in contrast to the other ligand-field components. This behavior has been observed in numerous Yb^{3+} containing ionic systems.[20] The $^2F_{5/2}(0') \rightarrow {}^2F_{7/2}(0)$ line in the luminescence spectrum of the crystal suffers from reabsorption. The total ligand-field splittings for the ground and excited states are 348 and 268 cm^{-1}, respectively. The 15 K $^2F_{5/2} \rightarrow {}^2F_{7/2}$ luminescence lifetime is 2.5 μs in the crystal. The luminescence intensity of the crystal decreases by about 50% between 15 and 125 K. At room temperature, the intensity is reduced by several orders of magnitude.

(20) Buchanan, R. A.; Wickersheim, K. A.; Pearson, J. J.; Herrmann, G. F. *Phys. Rev.* **1967**, *159*, 245−251.

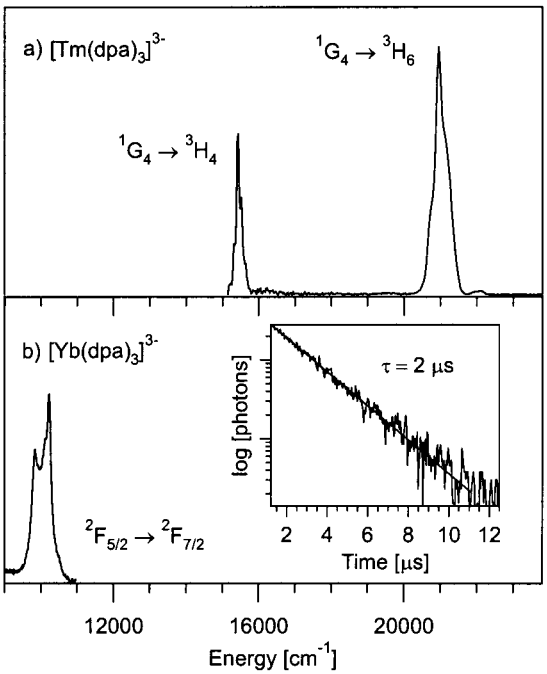

Figure 5. Luminescence spectra of aqueous solutions of $[Tm(dpa)_3]^{3-}$ (a) and $[Yb(dpa)_3]^{3-}$ (b) exciting into a ligand-centered level at 37026 cm^{-1}. The inset in (b) shows the luminescence decay curve of $[Yb(dpa)_3]^{3-}$ in a semilogarithmic representation. The resulting decay time is 2 μs.

The dpa complex of Yb^{3+} exhibits very weak near-infrared luminescence in solution at room temperature by exciting resonantly into the $^2F_{5/2}$ level at 10513 cm^{-1} or into the $^1\Pi-{}^1\Pi^*$ absorption band centered at 37026 cm^{-1}. This is shown in Figure 5b, where three maxima at 10224, 10112, and 9832 cm^{-1} can be identified. The inset to Figure 5b shows the temporal behavior of the luminescence intensity after 10 ns pulse excitation at 10312 cm^{-1}. The lifetime is 2 μs.

The same excitation at 37026 cm^{-1} in an aqueous solution of $[Tm(dpa)_3]^{3-}$ leads to blue and red luminescence, as shown in Figure 5a. The two bands at 20960 and 15430 cm^{-1} are readily assigned to transitions from the $^1G_4$ level to the ground state $^3H_6$ and to the first excited state $^3H_4$, respectively. The intensity ratio between these two bands is 3.5. An upper limit of <0.5 μs has been determined for the lifetime of $^1G_4$ at room temperature. Both transitions are also observed by directly exciting the $^1D_2$ level of Tm^{3+} at 27770 cm^{-1} or by resonant $^1G_4$ excitation with the 476.5 nm Ar^+ laser line. Excitation into the ligand at 37026 cm^{-1} additionally results in weak $^1D_2 \rightarrow {}^3H_4$ luminescence centered at 22000 cm^{-1}. Luminescence from the $^1G_4$ state is also observed in doped $[Tm(dpa)_3]^{3-}$ PVA matrixes at room temperature. Laser excitation at 476.5 nm into a single crystal of $Na_3[Tm(dpa)_3]\cdot 13H_2O$ leads to a broad band emission extending from 13500 to 21000 cm^{-1} and exhibiting reabsorption peaks corresponding to f−f excitations of Tm^{3+}. An upper limit of the lifetime at 15 K is 0.5 μs.

The 12834 cm^{-1} excitation at 15 K of $Na_3[Tm(dpa)_3]\cdot 13H_2O$ leads to highly resolved near-IR emission from the $^3F_4$ level. Figure 6 shows the 15 K $^3F_4 \rightarrow {}^3H_6$ luminescence and the corresponding excitation spectrum in comparison with the absorption spectrum in the same spectral region.

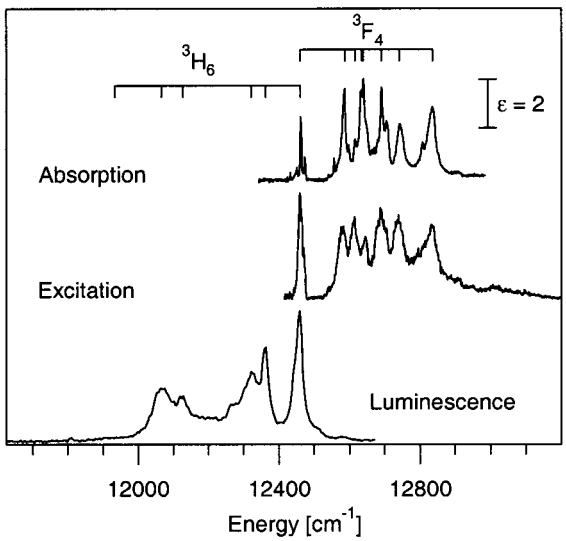

Figure 6. Absorption, luminescence, and excitation spectra of the $^3F_4 \leftrightarrow {}^3H_6$ transitions in a single crystal of $Na_3[Tm(dpa)_3]\cdot 13H_2O$ at 15 K. The luminescence was excited at 12834 cm^{-1}, and for the excitation spectrum, the luminescence was monitored at 12362 cm^{-1}. The electronic origins of some crystal-field levels are indicated at the top. ϵ is given in units of $[l\cdot mole^{-1}\cdot cm^{-1}]$.

Table 1. Experimental Luminescence Lifetimes

$[Yb(dpa)_3]^{3-}$ solution, 300 K	2 μs
$Na_3[Yb(dpa)_3]\cdot 13H_2O$, 15 K	2.5 μs
$Na_3[Tm(dpa)_3]\cdot 13H_2O$, 15 K (both, $^1G_4$ and $^3F_4$)	<0.5 μs
$[Tm(dpa)_3]^{3-}$ solution, 300 K ($^1G_4$)	<0.5 μs

The absorption spectrum closely follows the excitation spectrum, and we conclude that the luminescence is intrinsic. The resolution of the luminescence spectrum is instrumentally limited, and not all the ligand-field components can be identified. The excitation and absorption spectra are better resolved, and a reliable picture of the ligand-field splitting of the $^3F_4$ excited state can be derived. Total ligand-field splittings of 529 and 374 cm^{-1} are obtained for $^3H_6$ and $^3F_4$, respectively. Both in absorption and luminescence, we observe a physical broadening of the lines as we move away from the 0−0′ origin. This phenomenon is well-known in the high-resolution spectroscopy of f−f transitions. Its origin is an interaction of electronic origins with vibrational sidebands built on other origins. There is a sharp decrease in luminescence intensity with increasing temperature. For the lifetime at 15 K, an upper limit of <0.5 μs can be given. No resonant near-infrared luminescence was observed by exciting the Er^{3+}-centered $^4I_{11/2}$ level of a $Na_3[Er(dpa)_3]\cdot 13H_2O$ single crystal, even at cryogenic temperatures. The numerical values of all the measured luminescence lifetimes are collected in Table 1.

4. Discussion

4.1. Ligand- and Metal-Centered Excitations. The 2,6-pyridinedicarboxylic acid (H_2dpa) ligand was chosen for our study, because it was shown for dpa coordinated complexes of Eu^{3+},[21] Tb^{3+},[22] and Tm^{3+} [23] that in the $[Ln(dpa)_3]^{3-}$ complexes the f−f excitations were reasonably well shielded from the C−H and O−H oscillators of the ligands and the solvent. This is essential for the observation of f−f luminescence from molecular complexes. The absorption spectrum depicted in Figure 1 for a 0.14 mM solution of $[Yb(dpa)_3]^{3-}$ shows the typical spin-allowed $^1\Pi-{}^1\Pi^*$ excitations between 35000 and 40000 cm^{-1}. This part of the spectrum is essentially the same for the $[Tb(dpa)_3]^{3-}$ complex[22] and is very similar to the spectrum of the free ligand.[24] The $^1\Pi-{}^1\Pi^*$ excitations of the conjugated π system in dpa are practically unaffected by the lanthanide coordination.

There is no evidence of $^1\Pi-{}^3\Pi^*$ absorptions in the solution or crystal absorption spectra (see Figure 2), even at cryogenic temperatures. The lowest $^3\Pi^*$ level has been estimated to lie around 26600 cm^{-1} in $[Tm(dpa)_3]^{3-}$.[23] Despite the heavy-atom effect which can increase the $^1\Pi-{}^3\Pi^*$ oscillator strength by orders of magnitude, these transitions are still too weak to be observed in absorption. The relevance of ligand $^3\Pi^*$ excited states will become apparent in section 4.3, where excitation migration and excitation trapping are discussed.

The highly resolved crystal absorption spectra at cryogenic temperatures in Figures 2 and 3 contain a great deal of information about the f−f energy level structure and the intensity distribution among the f−f excitations. As described in section 3, assignments of the multiplets are straightforward. The $Na_3[Yb(dpa)_3]\cdot 13H_2O$ absorption spectrum only contains one multiplet just above 10000 cm^{-1} (see Figure 3), with the rest of the NIR, VIS, and near-UV transparent. This property of Yb^{3+}, which is due to its $4f^{13}$ configuration, makes this ion a very important one for various photonic applications in ionic crystals and glasses.[16,25]

When we use terms such as ligand-centered and lanthanide-centered excitations, we imply that the two types of excitations are decoupled. The justification for this lies in their vastly different oscillator strengths, combined with different energies. The $^1\Pi-{}^1\Pi^*$ transitions have typical oscillator strengths of the order of 0.1, whereas those of the f−f transitions are typically of the order of 10^{-6}, that is, 5 orders of magnitude smaller. This is mainly due to the shielding of the f-electrons resulting in atom-like behavior. In analogous transition metal ion complexes such as the $4d^6$ tris-chelate complex $[Ru(bpy)_3]^{2+}$, one also uses the terms ligand-centered and metal-centered for the excited states. But here, the distinction is not as clear-cut, because there are close-lying charge-transfer states, which mediate and lead to a certain mixing of the character.

4.2. Energy Transfer and Relaxation within the Complexes. The most efficient way to electronically excite the title complexes is by near-UV excitation into the $^1\Pi-{}^1\Pi^*$ absorptions around 37000 cm^{-1}. Nonradiative processes then

(21) Hopkins, T. A.; Bolender, J. P.; Metcalf, D. H.; Richarson, S. F. *Inorg. Chem.* **1996**, *35*, 5347−5355.
(22) Miller, T. L.; Senkfor, S. I. *Anal. Chem.* **1982**, *54*, 2022−2025.
(23) Sharma, P. K.; van Doorn, A. R.; Staring, A. G. J. *J. Lumin.* **1994**, *62*, 219−225.
(24) Peral, F.; Gallego, E. *Spectochim. Acta A* **2000**, *56*, 2149−2155.
(25) Shionoya, S.; Yen, W. M. *Phosphor Handbook*, Phosphor Research Society; CRC Press: Washington, DC, 1999.

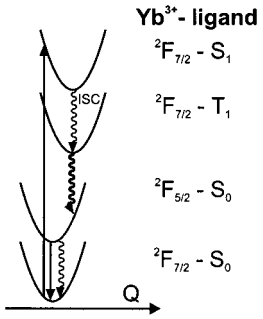

Figure 7. Single-configurational coordinate picture representing the nonradiative (curly arrows) and the radiative (straight arrows) relaxation channels in $[Yb(dpa)_3]^{3-}$. Q represents a breathing mode of the ligand of approximately 1200 cm^{-1}. The states are labeled in a double (Yb^{3+}−ligand) notation.

lead to the population of the lower-lying f−f excited states, and for $Na_3[Tm(dpa)_3]\cdot 13H_2O$ and $Na_3[Yb(dpa)_3]\cdot 13H_2O$, the f−f emissions in Figure 5 can be observed. This principle of intramolecular energy transfer has been described for a large number of lanthanide complexes with π chelate ligands.[1] As shown in Figure 7, an intraligand intersystem crossing (ISC) process from $^1\Pi^*(S_1)$ to $^3\Pi^*(T_1)$ is usually assumed to be the first step in this sequence. Compared to the free ligand, intersystem crossing is much more competitive against fluorescence in a lanthanide complex because of spin−orbit coupling induced by the heavy metal. We do not observe any ligand fluorescence in our complexes in solution. So, we take this first step as established.

The next step is usually called an energy transfer step from the ligand to the metal within a given complex. As such, it requires some spectral overlap between the luminescence profile, that is, the ligand phosphorescence profile in our system, and some lanthanide f−f absorption. With a lowest estimated $^3\Pi^*$ level around 26600 cm^{-1}, we can see from Figure 2 that the $^2H_{9/2}$ level of Er^{3+} around 24000 cm^{-1} is ideally suited for a resonant energy transfer, the $^1G_4$ level of Tm^{3+} around 21000 cm^{-1} may still have some overlap with the phosphorescence profile, and, in the case of the $^2F_{5/2}$ level of Yb^{3+} around 10000 cm^{-1}, there is definitely no spectral overlap with the ligand luminescence profile. This energy transfer step is usually considered to be efficient,[26] but it certainly calls for an explanation in the case of $[Yb(dpa)_3]^{3-}$ with an energy mismatch of about 16600 cm^{-1} between the lowest $^3\Pi^*$ level and the $^2F_{5/2}$ level of Yb^{3+}. A similar observation was recently reported for a Yb^{3+}−protein complex, in which excitation of the peptide group around 35000 cm^{-1} was found to lead to Yb^{3+} $^2F_{5/2}$ luminescence in the NIR. An electron transfer mechanism involving a Yb^{3+}/Yb^{2+} redox process was postulated to explain the puzzling result.[27] It is not plausible that such a mechanism should be active in $[Yb(dpa)_3]^{3-}$. Better guidance to an understanding of the phenomenon is found in a paper by Crosby and Kasha in the 1950s.[28]

Translated into modern language, this work postulates a phonon assisted energy transfer process, in which the excess energy is transformed into vibrational energy and ultimately heat. We translate this further into a single-configurational coordinate (SCC) picture. The situation can then be represented as shown in Figure 7, where the bold curly arrow represents the process we are discussing. It is important to realize that we have both ligand-centered and metal-centered states in the same diagram. We are, thus, using double labels to emphasize this. The step is no longer an energy transfer process from one chromophore (ligand) to another chromophore (Yb^{3+}). It is a nonradiative relaxation process from a highly excited state of the same chromophore, that is, the $[Yb(dpa)_3]^{3-}$ complex. The configurational coordinate Q in Figure 7 is the main expansion coordinate of the $\pi-\pi^*$ excitation, that is, essentially the breathing mode of the chelate ring. Within the Condon approximation, the nonradiative relaxation rate between two states $|b\rangle \rightarrow |a\rangle$ is proportional to a thermally averaged Franck−Condon factor. Within the SCC model at low temperatures, this is given by[29]

$$FC_{(T=0)} = |\langle \chi_{a,p} | \chi_{b,o} \rangle|^2 = \frac{e^{-S} S^p}{p!} \qquad (1)$$

where S is the Huang−Rhys factor, a measure of the displacement of the upper state $|b\rangle$ with respect to the lower state $|a\rangle$ along the coordinate Q; p is the reduced energy gap (in units of $\hbar\omega_Q$ between the $v=0$ levels of $|a\rangle$ and $|b\rangle$). For $[Yb(dpa)_3]^{3-}$, we can estimate $\hbar\omega_Q$ and S from the absorption spectrum in Figure 1; $\hbar\omega_Q \simeq 1200$ cm^{-1}, and $S \simeq 2$. From this, we immediately get $p \simeq 14$ for the ($^2F_{7/2}-T_1$) → ($^2F_{5/2}-S_0$) and $p \simeq 22$ for the ($^2F_{7/2}-T_1$) → ($^2F_{7/2}-S_0$) relaxation. The latter roughly corresponds to the $T_1 \rightarrow S_0$ nonradiative relaxation in the free ligand. In conjugated π systems at room temperature, typically between 1% and 50% of the $\pi-\pi^*$ excitation is lost nonradiatively. Applying eq 1, we calculate that the rate constant of the nonradiative ($^2F_{7/2}-T_1$) → ($^2F_{5/2}-S_0$) process in $[Yb(dpa)_3]^{3-}$ is 7 orders of magnitude bigger than that for $T_1 \rightarrow S_0$ in the free ligand. It is, thus, plausible that the nonradiative process shown with the bold curly arrow in Figure 7 is dominant. We conclude that the simple SCC picture with the full complex as the chromophore is better suited to understand this nonradiative step than the picture of an energy transfer with large mismatch between two separate chromophores.

We finally have to discuss the nonradiative relaxation processes between the metal-centered f−f states. Within an SCC picture, there is essentially no displacement of these states along any coordinate: we are in the weak coupling limit, that is, $S \simeq 0$. In this situation, the energy gap law very successfully accounts for the situation[30]:

(26) Klink, S. I.; Alink, P. O.; Grave, L.; Peters, F. G. A.; Hofstraat, J. W.; Geurts, F.; van Veggel, F. C. J. M. *J. Chem. Soc., Perkin Trans. 2* **2001**, 363−372.
(27) Horrocks, W. D., Jr.; Bolender, P. J.; Smith, W. D.; Supkowski, R. M. *J. Am. Chem. Soc.* **1997**, *119*, 5972−5973.
(28) Crosby, G. A.; Kasha, M. *Spectrochim. Acta* **1958**, *10*, 377−382.
(29) Brunold, T. C.; Güdel, H. U. In *Inorganic Electronic Structure and Spectroscopy*; Solomon, E. I., Lever, A. B. P., Eds.; Wiley: New York, 1999; pp 259−306.
(30) van Dijk, J. M. F.; Schuurmans, M. F. H. *J. Chem. Phys* **1983**, *78*, 5317−5323.

$$k_{nr} \sim e^{-\beta p} \quad (2)$$

The nonradiative relaxation rate constant decreases exponentially with increasing energy gap. In ionic crystals, p refers to the highest-energy vibrational mode $\hbar\omega_{max}$, and β is a specific constant of the material. There is a good rule of thumb in f-electron systems that nonradiative relaxation is dominant when the reduced energy gap to the next lowest level is $p \leq 5$. For a complex such as $[Ln(dpa)_3]^{3-}$, the highest-energy oscillators ($\hbar\omega_{max} \geq 3000$ cm^{-1}) have been purposely moved away from the metal ion, so that the breathing mode of the chelate ring ($\hbar\omega \simeq 1200$ cm^{-1}) may also participate in the deactivation. We, therefore, define and roughly estimate an effective vibrational energy $\hbar\omega_{eff} \sim 2000$ cm^{-1}, corresponding to a weighted average of the vibrations participating in the nonradiative relaxation process.

With this, we can interpret the observed behavior in the three complexes of this study. In $[Er(dpa)_3]^{3-}$, the largest energy gap between two adjacent energy levels above $^4I_{13/2}$ is about 4000 cm^{-1}, namely between $^4S_{3/2}$ and $^4F_{9/2}$; see Figure 2. The maximum p_{eff} is thus about 2, nonradiative relaxation dominates throughout, and no luminescence is observed. In $[Tm(dpa)_3]^{3-}$, the $^1G_4$ to $^3F_2$ energy gap is about 6000 cm^{-1}, and the gap between $^3F_4$ and $^3H_5$ about 4500 cm^{-1}; see Figure 2. This corresponds to p_{eff} values of 3.0 and 2.25 in our rough energy gap law estimate. Extremely weak luminescence with a lifetime shorter than 0.5 μs could be observed from both $^1G_4$ and $^3F_4$ in $[Tm(dpa)_3]^{3-}$; see Table 1. From studies of Tm^{3+} in ionic halide crystals, the lifetimes of $^1G_4$ and $^3F_4$ are known to be of the order of 0.5 and 1 ms, respectively.[31] We can assume that these decay times are radiative. We conclude that in $[Tm(dpa)_3]^{3-}$nonradiative depletion processes dominate the radiative luminescence processes from these states by a factor of at least 10^3.

In $[Yb(dpa)_3]^{3-}$, the luminescence intensity is clearly higher than in $[Tm(dpa)_3]^{3-}$. We determined the following lifetimes: 2 μs for $[Yb(dpa)_3]^{3-}$ in aqueous solution at room temperature and 2.5 μs for $Na_3[Yb(dpa)_3]\cdot 13H_2O$ at 15 K; see inset to Figure 5b and Table 1. In this case, the radiative lifetime of $^2F_{5/2}$ is about 1 ms. Therefore, nonradiative depletion processes dominate the radiative luminescence processes by a factor of about 5×10^2. We also note from the measured lifetimes in the Yb^{3+} samples that the nonradiative relaxation rate is essentially temperature independent. This is in contrast to the behavior of k_{nr} for energy gaps of $p = 5$ in chloride and bromide crystals.[13] The reason is that in our molecular system $\hbar\omega_{eff} \gg kT$ at all temperatures, whereas in the halides $\hbar\omega_{max}$ is of the same order of magnitude as kT at room temperature. In this discussion, we have not explicitly considered the influence of the solvent vibrations on the nonradiative deactivation of the complex. It has been shown for other encapsulated Yb^{3+} complexes that such an influence exists.[4] We have implicitly considered this influence in our estimate of $\hbar\omega_{eff} \sim 2000$ cm^{-1}. For the same complex in D_2O instead of H_2O, $\hbar\omega_{eff}$ would be correspondingly smaller.

4.3. Ligand-Field Splittings in $Na_3[Tm(dpa)_3]\cdot 13H_2O$ and $Na_3[Yb(dpa)_3]\cdot 13H_2O$. High-resolution absorption and luminescence spectroscopy has been used to determine crystal-field splittings of electronic multiplets in a large number of Ln^{3+} doped crystals.[32] In particular for laser crystals, a knowledge of the energy levels is very important. In the present study, we wanted to find out whether the high-resolution techniques could also yield information on ligand-field splittings in the molecular title complexes.

The 12 K crystal absorption spectra in Figure 2 show splittings of the multiplets even under moderate instrumental resolution, which are due to ligand-field splittings. By increasing the instrumental resolution, the natural line widths can be obtained, and they are of the order of 5 cm^{-1} at 15 K for the electronic origins. These line widths are inhomogeneous at this temperature.

A fundamental difference between ionic crystals containing lanthanide ions and the crystals containing ligands with conjugated π electrons becomes apparent when the crystals are excited in the green, blue, and near-UV regions. The title compounds all show a strong white luminescence covering the whole visible range at all temperatures. This is ascribed to the excitonic character of the $\pi-\pi^*$ excitations in the crystal. One consequence of this is that the lowest intrinsic $^1\Pi^*$ and $^3\Pi^*$ states of the crystal will lie below those of the isolated complex. Another consequence is the delocalization of the excitation, leading to a high probability of trapping by slightly perturbed or photochemically modified complexes and the consequent observation of luminescence from many traps covering a very broad spectral range.

Excitation below 14600 cm^{-1} is free of these complications, and we made use of the tunable Ti:sapphire laser to selectively excite the $^3F_4$ multiplet around 12500 cm^{-1} in $Na_3[Tm(dpa)_3]\cdot 13H_2O$ and the $^2F_{5/2}$ multiplet around 10200 cm^{-1} in $Na_3[Yb(dpa)_3]\cdot 13H_2O$.

We first discuss the fine structure of the $^2F_{7/2} \rightarrow {}^2F_{5/2}$ transitions in the latter. The high-resolution absorption spectrum is shown as a function of temperature in Figure 3, whereas the corresponding luminescence and laser excitation spectra at 15 K are depicted in Figure 4. From the fact that the absorption and the excitation spectra are identical, we conclude that the luminescence is intrinsic. The line at 10217 cm^{-1} is immediately identified as the $0-0'$ transition, that is, the common origin of both the absorption and the luminescence spectrum at low temperatures. In luminescence, this origin suffers from reabsorption in the crystal at low temperature and is thus reduced in intensity. The assignment of the other lines to the ligand-field components is shown at the top of Figures 3 and 4. It is complicated by the presence of relatively strong vibrational sidebands built on the $0-0'$ origin, both in absorption and luminescence. This phenomenon has been observed in the corresponding spectra of Yb^{3+} in many host lattices. It appears to be unique to Yb^{3+} and must have to do with its electronic structure. Nevertheless, by combining all the information from luminescence, excita-

(31) Özen, G.; Kermaoui, A.; Denis, J. P.; Wu, X.; Pelle, F.; Blanzat, B. *J. Lumin.* **1995**, *63*, 85−96.

(32) Lüthi, S. R.; Hehlen, M. P.; Güdel, H. U. *J. Chem. Phys.* **1999**, *110*, 12033−12043.

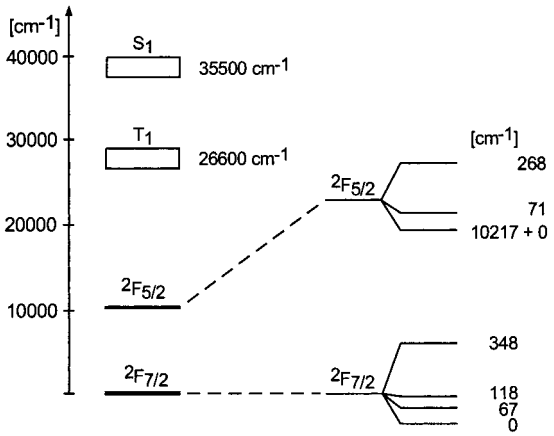

Figure 8. Schematic energy level diagram for a single crystal of $Na_3[Yb(dpa)_3]\cdot 13H_2O$. The energies (in wavenumbers) for S_1 and T_1 correspond to the estimated electronic origins.

tion, and temperature dependent absorption, we can confidently draw the energy level patterns for $^2F_{7/2}$ and $^2F_{5/2}$ as shown in Figure 8. Figure 4 also shows the 15 K luminescence and excitation spectra of $[Yb(dpa)_3]^{3-}$ in a PVA matrix. The band positions are the same as in the crystal spectrum, but they are inhomogeneously broadened.

In a very similar procedure, we analyze the 15 K absorption, luminescence, and excitation spectra of the $^3H_6 \leftrightarrow {}^3F_4$ transitions in $Na_3[Tm(dpa)_3]\cdot 13H_2O$. The 15 K absorption and excitation spectra are again similar, and there is a coincidence of the origins $0-0'$ at 12459 cm^{-1}. We conclude that the luminescence is intrinsic. Whereas at least six ligand-field components of $^3F_4$ can be identified from the absorption and excitation spectra, not all the ligand-field components of the $^3H_6$ ground state are resolved in the luminescence spectrum, and the energy level pattern for $^3H_6$ at the top of Figure 6 is thus incomplete. But again, these highly resolved spectra provide a good basis for a derivation of the ligand-field splittings in the ground and excited state.

The molecular symmetry of the $[Ln(dpa)_3]^{3-}$ complexes is D_3. In the monoclinic structure, space group $P2_1/c$, which all the title compounds adopt, the packing leads to small molecular distortions, and the exact point symmetry of the Ln^{3+} center is C_1. In the approximate point group D_3, we expect 4 and 3 ligand-field levels for $^2F_{7/2}$ and $^2F_{5/2}$ in $Na_3[Yb(dpa)_3]\cdot 13H_2O$, as observed and assigned. In $Na_3[Tm(dpa)_3]\cdot 13H_2O$, we expect 9 and 13 levels for $^3F_4$ and $^3H_6$, respectively, both in D_3 and C_1.

5. Conclusions

Excitation of $^1\Pi-{}^1\Pi^*$ transitions of the ligand is followed by efficient energy transfer to f−f excited states in all three title complexes in solution. The transfer process to the $^2F_{5/2}$ state of Yb^{3+}, which appears puzzling at first sight, can be plausibly explained using a simple SCC model and considering the whole $[Yb(dpa)_3]^{3-}$ complex as the relevant chromophore. Nonradiative relaxation processes are dominant also among the f−f excited states in all three systems. The result is that no luminescence could be observed for $[Er(dpa)_3]^{3-}$, and the luminescences of $[Tm(dpa)_3]^{3-}$ and $[Yb(dpa)_3]^{3-}$ are very weak and short-lived. There is no chance to induce and observe upconversion luminescence in these molecular compounds. Crystals excited in the green, blue, and near-UV regions show intense $\pi-\pi^*$ luminescence throughout the visible. This is ascribed to the excitonic character of the $\pi-\pi^*$ excitations, resulting in trap luminescence from impurities and photoproducts. On the other hand, by using high-resolution laser spectroscopy at cryogenic temperatures in the NIR, the crystal spectra can be used to determine the ligand-field splitting of the low-lying states in the Tm^{3+} and Yb^{3+} complexes.

Acknowledgment. We thank K. Krämer for his help with the X-ray diffraction characterization. This work was financially supported by the Swiss National Science Foundation.

IC0108484